Iranian Journal of Medical Physics
Vol. 9, No. 2, Spring 2012, 93-102
Received: April 14, 2012; Accepted: July 10, 2012

Original Article

The Monte Carlo Assessment of Photon Organ Doses from ^{222}Rn Progeny in Adult ORNL Phantom

Shila Banari Bahnamiri[1*], Reza Izadi Najafabadi[1], Seyed Hashem Miri Hakimabad[1]

Abstract

Introduction
The potential hazards posed by exposure to radiation from radon have been of great concern worldwide, since it is especially associated with increased risk of lung cancer. Some radioisotopes of radon progeny deposited in the human lungs emit β particles followed by the γ rays. While γ rays are comparatively less damaging to the respiratory system than α and β particles, it is the principal deposited energy in other organs.
Materials and Methods
In order to establish a quantitative estimate of hazards caused by the radiation, this paper studies the photon absorbed doses from radon progeny in all major organs of the human body through a simulation of the Oak Ridge National Laboratory (ORNL) adult phantom using MCNPX2.4.0 Monte Carlo code and calculations which were performed in photon/electron mode.
Results
Effective dose due to photons from radon progeny deposited in the human lungs was about 1.69 $\mu SvWLM^{-1}$. Based on UNSCEAR2006 reports, the effective dose of these photons per year is about 5.76×10^{-1}mSv in for radon concentration of 31000 Bq/m^3 (the maximum concentration of radon in Iran). Therefore, this value is comparable with 1mSv (The annual allowable effective dose).
Conclusion
The dosimetry of photons particularly in areas with high levels of exposure to radon and radon's decay products is important because all organs receive the photon absorbed dose from radon progeny.
Keywords: Dosimetry, Lung Cancer, ORNL Phantom, Radon Progeny, MCNPX

1- Physics Department, Faculty of Science, Ferdowsi University of Mashhad, Mashhad, Iran
*Corresponding author: Tel: 0912 585 6675; Email: shila_banari@yahoo.com

1. Introduction

The radiation dose from ^{222}Rn, which is a radioactive transformation product of ^{238}U, is the main natural dose received by the mankind. It exists in varying concentrations in all types of soil, minerals, ground water, building materials, and air [1]. The association between ^{222}Rn exposure and lung cancer has already been demonstrated in epidemiological studies performed on cohorts of miners [2].

^{220}Rn, or thoron from the ^{232}Th series, and ^{219}Rn from ^{235}U have very short lives (55.6 s and 3.96 s, respectively) and they are of minor significance compared with ^{222}Rn in 238U series. The half-life of ^{222}Rn (3.82 day) is long enough to diffuse into and build up in homes [3]. Natural level of ^{222}Rn in open space is usually below 10 Bq.m-3 [4]. In the closed space, ^{222}Rn can accumulate due to poor air ventilation.

Radon and its progenies enter the human respiratory tract system through inhalation. Being an inert gas, radon is not deposited in the human airways. Therefore, it is quickly exhaled. However, radon progeny are electrically charged and the particles easily deposit in the lungs (on the surface of the respiratory tract) after inhalation. Because of their relatively short half-lives (less than 1 hour), the radon daughters (α, β, γ, and X-ray) will decay mainly in the airways before being cleared either by absorption into blood or by particle transport to the gastrointestinal tract [2].

Photons emitted by ^{214}Bi and ^{214}Pb contribute negligibly to the amount of energy deposited in the human respiratory system in comparison with α and β particles. However, the absorbed doses of photons in lungs in respect to other organs are dominant because initial energies of photons are largest in lungs and the photons deposit largest energies than in other organs.

The most accurate way for estimating the absorbed dose is using Monte Carlo method, in which the processes, physical systems, and phenomena are simulated by statistical methods using random numbers [5].

In this work, the absorbed organ doses from γ radiations and X-rays emitted from radon progeny (^{214}Bi and ^{214}Pb) using modified ORNL analytical hermaphrodite phantom and MCNP code were estimated [6]. Besides, the effect of different radioactive decay data from two web-based libraries ENDF/VI [7] and LBNL/LUND table of radioactive isotopes [8] on organ dose values was analyzed.

2. Materials and Methods

2.1. Anthropomorphic Phantom

Direct measurement of absorbed dose in a human body is not generally possible. Therefore, anthropomorphic phantoms and Monte Carlo simulations are most commonly used for estimating the absorbed dose.

Analytical models of the human body (called human phantoms) were described in ORNL publications [9]. These phantoms are basically solid-geometry models that describe exterior and interior anatomical features of a human body using analytical equations. Human phantom consists of three types of tissues: skeletal, lung, and soft, with different densities and elemental compositions [10].

Although the organ doses from γ rays emitted by radon progeny is in very low dose range, the effect of simulation quality on the accuracy of dose estimations is important. One of the organs, which it's shape and position may have an effect on the results, is thyroid. Therefore, two geometric models of the thyroid were simulated. The results of this comparison would imply the significance of employing a model with secure high accuracy.

2.2. Thyroid Models

Since the thyroid is a very sensitive part of the human body, several mathematical relationships are available to define the thyroid cell in the input file of phantoms for dosimetry calculations. In this study, the absorbed doses in two different geometries of thyroid were compared: ORNL model [9, 11] and Ulanovsky design [12-14].

The ORNL model of thyroid was proposed by Eckerman et al. in 1996 [9]. In this model, the thyroid is located in the neck, close to its front

surface and is composed of two lobes. These two lobes are represented as the volumes between two concentric cylinders cut by a fourth degree surface, two horizontal planes, and one vertical plane. Since this model contains surface equations that are higher than second order, the new equations which could be accommodated by MCNP were prepared by Krstic et al. [11] on the basis of previous one.

On the other hand, Ulanovsky et al. have developed a simplified mathematical model of the thyroid gland [15-13]. A schematic view of the thyroid models is shown in Figure 1. The neck in the model is represented by right circular cylinder and the thyroid by two lobes with an isthmus. Each lobe is described by a right ellipsoid cut by the tracheal cylinder. When compared with the ORNL phantom, the thyroid has been moved closer (about 3 cm) to the spine region. The total volume of the both thyroid models is 19.9 cm^3.

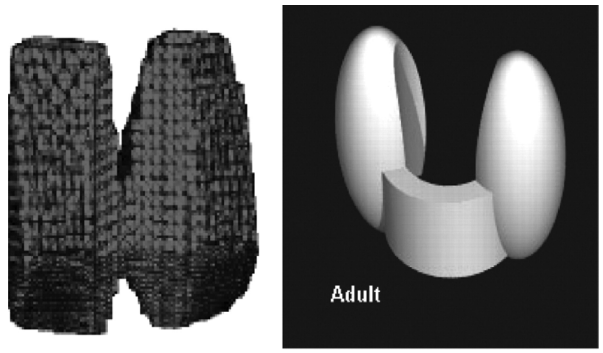

Figure 1. The schematics of (a) revised ORNL thyroid and (b) Ulanovsky thyroid phantom.

2.3. Dose Assessment

In order to calculate the doses in other sensitive organs when the source is in the lungs, ORNL phantom of the human body was used. Since the radon progeny attached to the aerosols in the air enter the lungs through inhalation and decay in the lungs, one can define the lungs as the main radiation source for input file of Monte Carlo N-Particle (MCNP) code.

Due to the high penetrability of γ, it is assumed as the uniform source of radiation. MCNP and Monte Carlo transport codes were used with the modified ORNL adult phantom to determine the doses from photon (γ radiation and X-ray) emitted from radon progeny (in MeV/gr per one particle of radiation).

+F6 tally calculates the absorbed dose by considering the photon/electron transport and utilizing the libraries prepared in the code. Calculations were performed on a personal computer with the following specifications: Pentium(R), 2.5 GHz processor, 2 GB RAM and 64-bit Windows 7. The cross sections used in this project were chosen from the ENDF/B-VI radioactive decay data [10]. The calculations were performed separately in four programs for γ radiation and X-ray emitted from ^{214}Pb and ^{214}Bi. The yields (Bq-s)$^{-1}$ versus energy (MeV) of X-ray and γ radiation for ^{214}Pb and ^{214}Bi were taken from LBNL/LUND and ENDF/VI decay data and are presented in Figures 2 and 3, respectively [10-12].

The energy lines and energy yield per one isotope (^{214}Pb, ^{214}Bi), were defined in SDEF card of input files. The output files of MCNP code were obtained from the mean absorbed dose (in MeV/g per one particle of radiation) in the ”main” organs and the ”remainder” tissue of the human body [5].

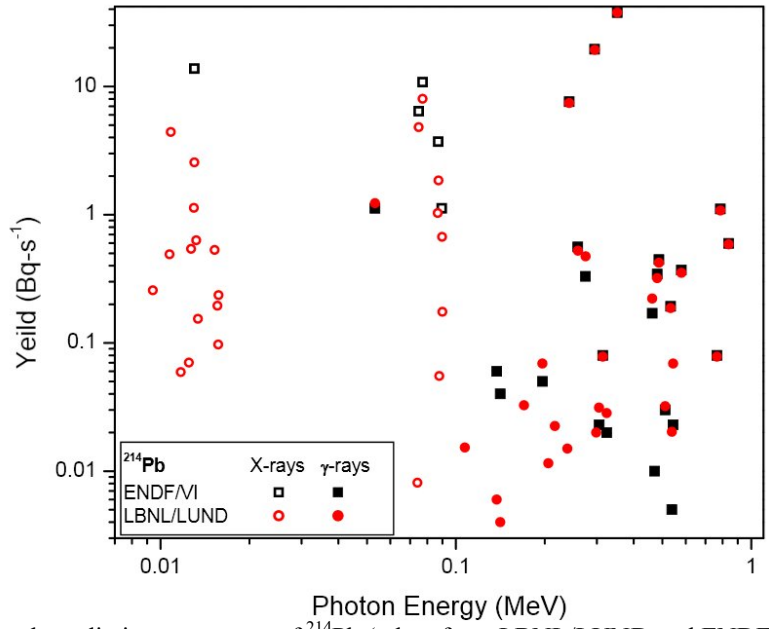

Figure 2. X-ray and γ radiation spectrums of ^{214}Pb (taken from LBNL/LUND and ENDF/VI decay data).

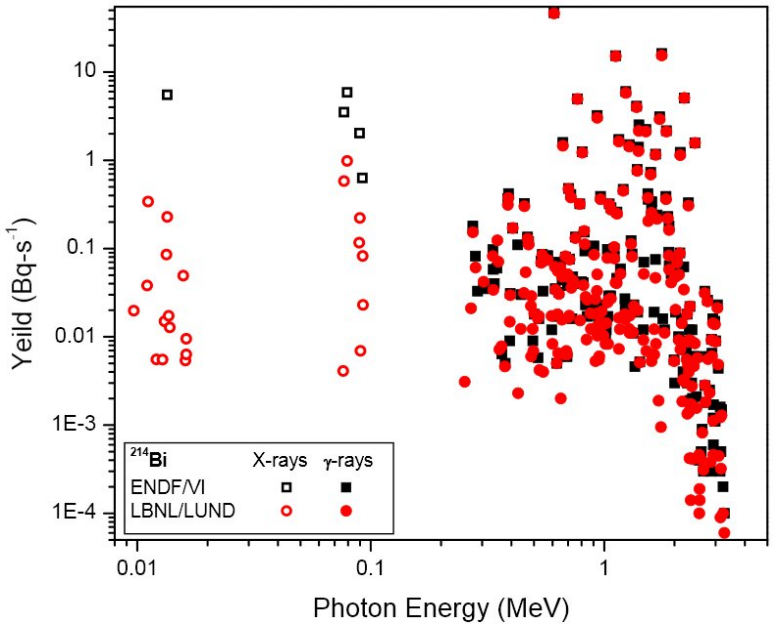

Figure 3. X-ray and γ radiation spectrums of ^{214}Bi (taken from LBNL/LUND and ENDF/VI decay data).

The averaged absorbed dose (MCNP output), $\overline{{}_{T}D_{R}^{n}}$, is the quotient of deposited energy due to radiation of type R in the volume of specific organ or tissue T by its mass from nuclide n (^{214}Pb or ^{214}Bi).

The mean absorbed dose per particle of radiation (in μGy WLM^{-1}) from whole lung as a source was calculated using Equation (1). Working level month (WLM)is exposure to the radon progeny of 1 WL ($2.08\times10^{-5} Jm^{-3}$) during 170 h.

$$ {}_{T}D_{R}^{n} = \overline{{}_{T}D_{R}^{n}}.A_{n}.I_{R}^{n} \qquad (1) $$

where, A_n is activity of each isotope (n) and I_R^n is the yield of radiation. Since $\overline{{}_{T}D_{R}^{n}}$ obtained in the simulation is given per quantum or per particle of radiation, and

activities per disintegration, to derive absorbed dose per 1 WLM, one needs to know the yield of certain type of radiation [5].

The yield of β is 1 while the yield for γ quanta is different, because one or more γ particles can be emitted per disintegration. The yield of ^{214}Pb γ spectrum is 0.704 (Bq-s)$^{-1}$, whereas that of ^{214}Bi is 1.364 (Bq-s)$^{-1}$. The yield of ^{214}Pb X-ray spectrum is 0.358 (Bq-s)$^{-1}$, whereas that of ^{214}Bi is 0.176 (Bq-s)$^{-1}$ [10]. For ^{214}Pb, the total activity in all regions is 406.8 Bq per 1 WL, while for ^{214}Bi, it is 578.4 Bq per 1 WL [5]. These are results from the program LUNGDOSE.F90. This program includes calculation working level month deposition of aerosols in different deposition regions of the Human Respiratory Tract Model (HRTM) according to the algebraic model of ICRP Publication 66 and equilibrium activities of radon progeny in different clearance regions of the HRTM and the total number of emitted particles for given exposure conditions and exposure time. The input parameters for the program LUNGDOSE.F90 are such as breathing rate of $0.78 m^3 h^{-1}$, equilibrium factor of 0.395 and these are very important parameters for calculating photon activity [5].

The absorbed doses were reported per 1 WLM in μGyWLM^{-1} using Equations (2) and (3).

$$ {}_T D_R^{214Pb} = {}_T D_\gamma^{214Pb} + {}_T D_{X-ray}^{214Pb} \quad (2) $$

$$ {}_T D_R^{214Bi} = {}_T D_\gamma^{214Bi} + {}_T D_{X-ray}^{214Bi} \quad (3) $$

Photon absorbed doses were estimated for 24 main organs. The equivalent dose H_T is one of the radiobiological protection quantities that is defined as a weighted mean absorbed dose, in some organ T, from γ and X-ray, and was obtained using Equation 4.

$$ H_T = \sum_n \sum_{X-ray,\gamma} w_R \ {}_T D_R^n \quad (4) $$

where, w_R is the radiation weighting factor which depends on the radiation type and energy whose values for photon radiations are equal to 1.

The effective dose, which is the main radiation protection quantity, is obtained using Equation (5). Sex averaged effective dose was calculated as:

$$ E_{eff} = \sum_T w_T \frac{H_{TM} + H_{TF}}{2} \quad (5) $$

Where, w_T is the tissue weighting factor taken from recent ICRP publication 103 [14]. H_{TM} and H_{TF} are the equivalent doses for male and female, respectively.

3. Results and Discussion

3.1. Organ Doses

All dosimetric quantities estimated in this work have an uncertainty less than 2%. ${}_T D_R^n$ Per WLM for γ radiation, and X-ray emitted from ^{214}Pb and/or ^{214}Bi in 24 main organs of the human body are showed in Table 1. These results were calculated by using ENDF/VI decay data. As expected, some of the photons emitted by radon progeny have enough energy to leave the lungs and deposit their energies in other organs, for which the organ doses cannot be disregarded.

In all cases, organ doses due to ^{214}Pb are lower by about 20% than that of ^{214}Bi because of significantly lower γ rays (of high energy and yield) in the γ spectrum of ^{214}Pb compared with ^{214}Bi.

As expected, the results show that the lungs being the organ that receives the highest absorbed dose. The second and third highest doses after lungs are received by heart and Esophagus, respectively, because both of them are located close to the lungs. The bladder receives lesser absorbed dose than other organs, as it is located farthest from the source. The X-rays absorbed dose due to ^{214}Bi can be considered negligible in comparison with γ absorbed dose because the former is less than 2% in comparison with the latter. The absorbed dose of X-ray in all other organs except for the bone surface and lungs is less than 1% of γ absorption dose. However, the X-ray absorption dose due to ^{214}Pb, especially in the lungs, is about 20% of γ absorbed dose, and in the bone surface it is about 17% of γ absorbed dose. Unlike ^{214}Bi, the X-ray absorption dose due to ^{214}Pb for most organs is not negligible compared with γ absorbed dose, because the dose is more than 5% of γ absorbed dose.

Table 1. Organ doses from γ radiation and X-ray from radon progeny nuclides, ^{214}Pb, and ^{214}Bi, distributed in the human lungs (in μGy WLM^{-1}) using ENDF/VI decay data.

Organs	^{214}Pb		^{214}Bi	
	γ-ray	X-ray	γ-ray	X-ray
Kidneys	3.15 E-02	2.31 E-03	2.80 E-01	1.85 E-03
Pancreas	7.35 E-02	6.74 E-03	5.79 E-01	5.34 E-03
Small Intestine	8.10 E-03	4.15 E-04	8.99 E-02	3.37 E-04
Adrenals	9.93 E-02	8.65 E-03	7.79 E-01	6.86 E-03
Gall Bladder	3.36 E-02	2.69 E-03	2.87 E-01	2.15 E-03
Heart	1.82 E-01	1.74 E-02	1.42 E+00	1.37 E-02
Skin	1.89 E-02	1.25 E-03	1.75 E-01	9.98 E-04
Thyroid	4.56 E-02	3.65 E-03	3.96 E-01	2.91 E-03
Stomach	5.19 E-02	4.51 E-03	4.27 E-01	3.58 E-03
Bone Surfaces	3.52 E-02	5.96 E-03	2.68 E-01	4.63 E-03
Lungs	4.91 E-01	9.77 E-02	3.88 E+00	6.47 E-02
Esophagus	1.80 E-01	1.66 E-02	1.38 E+00	1.31 E-02
Bladder	1.31 E-03	3.12 E-05	2.37 E-02	2.61 E-05
Thymus	1.22 E-01	1.14 E-02	9.72 E-01	8.99 E-03
Liver	8.51 E-02	7.80 E-03	6.73 E-01	6.16 E-03
Brain	3.62 E-03	1.34 E-04	4.92 E-02	1.09 E-04
Colon	6.68 E-03	3.53 E-04	7.48 E-02	2.87 E-04
Breast	1.04 E-01	8.36 E-03	8.65 E-01	6.61 E-03
Uterus	3.03 E-03	1.00 E-04	4.31 E-02	8.27 E-05
Ovaries	3.25 E-03	1.11 E-04	4.58 E-02	9.23 E-05
Testes	2.71 E-04	3.14 E-06	8.50 E-03	2.63 E-06
Red Bone Marrow	4.87 E-02	4.49 E-03	2.92 E-01	3.57 E-03
Muscle	3.99 E-02	3.63 E-03	3.26 E-01	2.83 E-03
Spleen	6.98 E-02	6.25 E-03	5.59 E-01	4.94 E-03

3.2. Decay Data Sheets

Table 2 shows the doses calculated for X-rays and γ rays from ^{214}Pb and ^{214}Bi using LBNL/LUND decay data sheets. The relative difference of the dose values from this decay data sheets from the ENDF/VI decay data is approximately less than 5% (Table 2). This shows that although there are significant differences between two decay data sheets, the yields are too small to make a significant effect on dosimetry calculations. Therefore, both data sets can be used in dosimetry calculations.

3.3. Thyroid Model

Dose values for two thyroid models were listed in Table 3. As can be seen, in the ORNL model, thyroid has received lower dose than Ulanovsky's by a factor of about 2. Difference in their location can at least partly explain this discrepancy. Such large disagreements between dosimetric data, which are originated from differences in shapes or positions of organs within the body is alarming. One has to be very cautious about the accuracy of these data when applied for a group of people. In a future work, we would consider the six age group phantoms together with some voxel models in order to obtain the dose uncertainty for radon and its progeny.

Table 2. Organ doses from γ radiation and X-ray from radon progeny nuclides, ^{214}Pb, and ^{214}Bi, distributed in the human lungs (in μGy WLM^{-1}) using LBNL/LUND decay data and the comparison with ENDF/VI results.

Organs	^{214}Pb		^{214}Bi	
	Organ Dose (μGy WLM^{-1})	Relative Difference	Organ Dose (μGy WLM^{-1})	Relative Difference
Kidneys	3.32 E-02	1.78%	2.70 E-01	4.26%
Pancreas	7.84 E-02	2.24%	5.59 E-01	4.28%
Small Intestine	8.40 E-03	1.29%	8.65 E-02	4.10%
Adrenals	1.06 E-01	1.85%	7.52 E-01	4.29%
Gall Bladder	3.55 E-02	2.20%	2.77 E-01	4.15%
Heart	1.95 E-01	2.26%	1.37 E+00	4.20%
Skin	1.98 E-02	1.49%	1.68 E-01	4.55%
Thyroid	4.83 E-02	2.03%	3.82 E-01	4.26%
Stomach	5.53 E-02	1.95%	4.12 E-01	4.18%
Bone Surfaces	3.96 E-02	3.65%	2.59 E-01	5.13%
Lungs	5.66 E-01	3.90%	3.75 E+00	5.06%
Esophagus	1.92 E-01	2.04%	1.33 E+00	4.32%
Bladder	1.32 E-03	1.49%	2.28 E-02	4.20%
Thymus	1.31 E-01	2.24%	9.39 E-01	4.28%
Liver	9.09 E-02	2.15%	6.49 E-01	4.42%
Brain	3.72 E-03	0.80%	4.73 E-02	4.06%
Colon	6.94 E-03	1.28%	7.20 E-02	4.13%
Breast	1.10 E-01	1.79%	8.35 E-01	4.24%
Uterus	3.11 E-03	0.64%	4.13 E-02	4.40%
Ovaries	3.36 E-03	0.0%	4.39 E-02	4.36%
Testes	2.68 E-04	2.19%	8.10 E-03	4.71%
Red Bone Marrow	5.20 E-02	2.22%	2.81 E-01	4.85%
Muscle	4.27 E-02	1.84%	3.15 E-01	4.41%
Spleen	7.45 E-02	2.10%	5.40 E-01	4.26%

Table 3. Comparison of thyroid absorbed doses (μGy WLM^{-1}) due to photons from ^{214}Pb and ^{214}Bi for ORNL and Ulanovsky models.

Thyroid model	^{214}Pb	^{214}Bi
ORNL	2.46E-02	2.07E-01
Ulanovsky	4.83E-02	3.82E-01

3.4. Effective Dose

Data in Table 4 shows the total absorbed dose (X-ray and gamma radiation) from radon progeny and the organs contribution in effective doses for male and female.

Based on these data, the whole body effective dose was obtained according to ICRP103 recommendation. The effective dose due to photons from radon progeny deposited in the human lungs was about 1.69 μSvWLM^{-1}.

Although the contribution of alpha particles (emitted from radon progeny) in effective dose is about 15 mSvWLM^{-1} [16], just lungs received their absorbed dose and alpha particles cannot be exhaled out of the lungs because of their short range. Photons contribution in effective dose is important because all organs received the photon absorbed dose from radon progeny.

UNSCEAR 2006 reported the radon concentration in Iran. The results showed the minimum and maximum concentration are $82\,Bq/m^3$ and $31000\,Bq/m^3$, respectively.

Based on these results, the effective dose per year (from photons) is $5.76\times10^{-1}\,mSv$ in $31000\,Bq/m^3$. Therefore, this value is comparable with $1\,mSv$ (The annual allowable effective dose) [17].

The annual organ absorbed dose for maximum and minimum concentration of radon are showed in Table 5. The results show the absorbed dose in some organs such as lungs, heart, esophagus, thymus, and breast are notable.

Table 4. Total organ doses from γ radiation and X-ray from radon progeny nuclides, ^{214}Pb, and ^{214}Bi in the human lungs (in μGy WLM^{-1}).

Organs	Total absorbed dose (D_{tot})	w_T	$D_{tot} \times w_T$
Kidneys	3.16E-01	0.12	3.79E-02
Pancreas	6.65E-01	0.12	7.98E-02
Small Intestine	9.87E-02	0.12	1.18E-02
Adrenals	8.94E-01	0.12	1.07E-01
Gall Bladder	3.26E-01	0.12	3.90E-02
Heart	1.63	0.12	1.95E-01
Skin	1.96E-01	0.01	1.96E-03
Thyroid	4.48E-01	0.04	1.79E-02
Stomach	4.87E-01	0.12	5.84E-02
Bone Surfaces	3.14E-01	0.01	3.14E-03
Lungs	4.54	0.12	5.44E-01
Esophagus	1.59	0.04	6.36E-02
Bladder	2.51E-02	0.04	1.00E-03
Thymus	1.12	0.12	1.34E-01
Liver	7.72E-01	0.04	3.09E-02
Brain	5.31E-02	0.01	5.31E-04
Colon	8.22E-02	0.12	9.86E-03
Breast	9.84E-01	0.12	1.18E-01
Uterus	4.63E-02	0.12	5.56E-03
Ovaries	4.92E-02	0.08	3.94E-03
Testes	8.78E-03	0.08	7.02E-04
Red Bone Marrow	3.48E-01	0.12	4.18E-02
Muscle	3.72E-01	0.12	4.47E-02
Spleen	6.40E-01	0.12	7.69E-02

Table 5. The annual absorbed dose of photon emitted from radon progeny based on UNSCEAR 2006 radon concentration measurement in Iran.

Oragans	Total absorbed dose $\mu GyWLM^{-1}$	Annual effective dose of photon from radon progeny $\mu Gy/year$	
		$82\,Bq/m^3$	$31000 Bq/m^3$
Kidneys	3.16E-01	2.84E-01	107.52
Pancreas	6.65E-01	5.99E-01	226.34
Small Intestine	9.87E-02	8.89E-02	33.61
Adrenals	8.94E-01	8.06E-01	304.48
Gall Bladder	3.26E-01	2.93E-01	110.82
Heart	1.63	1.47	554.40
Skin	1.96E-01	1.76E-01	66.61
Thyroid	4.48E-01	4.04E-01	152.65
Stomach	4.87E-01	4.38E-01	165.75
Bone Surfaces	3.14E-01	2.82E-01	106.79
Lungs	4.54	4.09	1544.99
Esophagus	1.59	1.43	541.85
Bladder	2.51E-02	2.26E-02	8.543
Thymus	1.12	1.00	379.70
Liver	7.72E-01	6.95E-01	262.84
Brain	5.31E-02	4.78E-02	18.08
Colon	8.22E-02	7.40E-02	27.97
Breast	9.84E-01	8.86E-01	335.08
Uterus	4.63E-02	4.17E-02	15.77
Ovaries	4.92E-02	4.43E-02	16.76
Testes	8.78E-03	7.91E-03	2.99
Red Bone Marrow	3.48E-01	3.14E-01	118.60
Muscle	3.72E-01	3.35E-01	126.76
Spleen	6.40E-01	5.77E-01	218.09

5. Conclusion

A detailed investigation on photon absorbed dose from ^{222}Rn progeny (^{214}Pb and ^{214}Bi) was performed by using Monte Carlo simulations and an adult phantom. The results show that the lungs are the source and receive the highest photon absorbed dose compared wih other organs.

Organ doses due to ^{214}Pb are lower than that of ^{214}Bi because of significantly lower γ rays (of high energy and yield) in the γ spectrum of ^{214}Pb compared with ^{214}Bi. The organ shape can also influence the dose. The comparison between data of two different models of thyroid indicates that the organ geometry can change dose values of the order by a factor of about 2. Moreover, two different data sets (LBNL/LUND and ENDF/VI) were examined, and the agreement between dosimetric data demonstrates that both of them can be used in dosimetry calculations.

The results show the photon absorbed dose in some organs such as lungs, heart, esophagus, thymus, and breasts are remarkable especially for the maximum concentration of radon in Iran according to UNSCEAR2006. The contribution of such great organ doses should be studied for lung, esophagus, and breast cancers particularly in high background radiation areas including the north of Iran.

Acknowledgment

This work was financially supported by the Ferdowsi University of Mashhad-Iran.

References

1. Nikezic D, Yu KN. Dosimetric model of human lung and associated computer programs. Indian J Phys. 2009; 83(6):759-75.
2. International Commission on Radiological Protection. Human Respiratory Model for Radiological Protection. Ann ICRP. 1994;24:1-120.
3. Martin JS. The Physics of Radiation Protection. Second, editor: John Wiley & Sons Canada, Limited; 2006.
4. Yu KN, Lau BM, Nikezic D. Assessment of environmental Radon hazard using human respiratory tract models. J Hazard Mater. 2006;132(1):98-110.
5. Markovic VM, Krstic D, Nikezic D. Gamma and beta doses in human organs due to radon progeny in human lung. Radiat Prot Dosimetry. 2009;135(3):197-202.
6. Eckerman KF, Cristy M. Ryman JC. The ORNL Mathematical Phantom Series, Informal Paper. Available from: http://homer.hsr.ornl.gov/VLab/mird2.pdf. Accessed Dec 15, 2008.
7. Hakimabad HM, Motavalli LR. Evaluation of specific absorbed fractions from internal photon sources in ORNL analytical adult phantom. Radiat Prot Dosimetry. 2008;128(4):427-31.
8. Ulanovsky AV, Minenko VF, Korneev SV. Influence of measurement geometry on the estimate of 131I activity in the thyroid: Monte Carlo simulation of a detector and a phantom. Health Phys. 1997;72(1):34-41.
9. Ulanovsky AV, Eckerman KF. Absorbed fractions for electron and photon emissions in the developing thyroid: fetus to five-years old. Radiat Prot Dosimetry. 1998;79(1-4):419-24.
10. Table of Radioactive Isotopes of ENDF/IV. Periodic Table linked to decay data for known isotopes of each element. http://t2.lanl.gov/data/decayd. html
11. International Commission on Radiological Protection. Recommendations of the International Commission on Radiological Protection. Ann ICRP. 2007;103:1-34.
12. Chart of Radioactive Nuclides. Available from http://ie.lbl.gov/education/isotopes.htm. Accessed Dec 15, 2008.
13. Input files with ORNL-mathematical phantoms of the human body for MCNP-4b. Available from http://www.pmf.kg.ac.yu/radijacionafizika/InputFiles.html. Accessed Dec 15, 2008.
14. Cristy M, Eckerman K.. Specific Absorbed Fractions of Energy at Various Ages from Internal Photon Sources; pp. V1–V7, ORNL/TM-8381, Oak Ridge, TN: Oak Ridge National Laboratory; 1987.
15. Briesmeister JF. MCNP - A general Monte Carlo N-Particle transports Code. Version 4C Ed. Los Alamos New Mexico: Los Alamos National Laboratory 2000.

16. Nikezic D, Yu KN. Micro dosimetric calculation of absorption fraction and the resulting dose conversion factor for radon progeny. Radiat Environ Biophys. 2001; 40(3):207–11.
17. Source and effect of ionizing radiation. New York: United Nations Scientific Committee on the Effect of Atomic Radiation. Available from: http://www.unscear.org/docs/reports/2008/09-86753_Report_2008_Annex_B.pdf. Accessed Aug 10, 2012.